

Enhancement of Water Permeation across a Nanochannel by the Structure outside the Channel

Xiaoqing Gong,^{1,2,3} Jingyuan Li,¹ He Zhang,⁴ Rongzheng Wan,¹ Hangjun Lu,⁵ Shen Wang,^{1,3} and Haiping Fang^{1,*}

¹Shanghai Institute of Applied Physics, Chinese Academy of Sciences, Shanghai 201800, China

²Suzhou Institute of Nano-tech and Nano-bionics, Chinese Academy of Sciences, Suzhou 215125, China

³Graduate School of the Chinese Academy of Sciences, Beijing 100080, China

⁴Department of Biology, Shanghai Jiaotong University, Shanghai 200240, China

⁵Department of Physics, Zhejiang Normal University, Jinhua 321004, China

(Received 17 June 2008; published 15 December 2008)

We used molecular dynamics simulation to study the effect of the external structure on water permeation across a single-walled nanochannel. In contrast with the macroscopic scenario, the outside structure greatly affects the water transport across the nanochannel. Remarkably, the ratio of maximal to minimal flux reached a value of about two for different outside structures. These findings are expected to be helpful in design of high-flux nanochannels and provide an insight into the contribution of the lipid membrane to water permeation across biological water channels.

DOI: 10.1103/PhysRevLett.101.257801

PACS numbers: 61.20.Ja

The dynamics of water across nanochannels has significant implications for both the understanding of biological activities [1] and the design of novel nanofluidic devices or machines, which have a wide range of potential applications [2]. As an example, Holt *et al.* found that the water flow rate through a carbon nanotube with a radius of 1 to 2 nm was more than 3 orders of magnitude faster than the nonslip, hydrodynamic flow as calculated from the Hagen-Poiseuille equation [3]. If this tube can be used in the desalination of seawater, the required energy is expected to be greatly reduced [4]. Simple nanochannels with appropriate radii have also been utilized as model systems in the exploitation of some primary behaviors of complex biological water channels [5–9]. The water molecules inside appropriate-radius carbon nanotubes share at least three characteristics with those inside biological channels: the single-file arrangement, wavelike density distribution, and wet-dry transition resulting from confinement [1,5–9].

In practical applications, the structure outside the nanochannel is usually indispensable. This structure is usually important in fixing the positions of the nanochannels, and ensures that the permeation of water is only facilitated through the nanochannels. Lipid bilayer membranes of living cells are efficient barriers to water and ions, with the result that the molecules can only be transported into or out of cells via protein channels [1]. In recent experiments [3] measuring gas and water flow through a microfabricated device with aligned carbon nanotubes as pores, silicon nitride was applied to fill the gaps between neighboring carbon nanotubes, which acted as an impermeable membrane.

However, how the structure outside the channel affects the permeation of fluid across nanochannels has rarely been discussed. It is widely accepted that the external structure of the system scarcely affects water permeation across a macroscopic channel [10]. The structure and

(wetting or dewetting) properties of the inner surface of the channel have received almost all the attention while other features are usually neglected. For nanoscale systems, the behaviors usually differ from what occurs on the macroscopic scale [5–11]. Recently, it was found that polar liquids (water, for example) flowing inside a single-walled carbon nanotube (SWNT) could drive the polar molecules adsorbed on the tube surfaces to move along its axial direction [12], showing that interactions between the water inside the single-walled channel and other molecules outside cannot be neglected.

In this Letter we present an approach that takes this interaction into account by using molecular-dynamics simulation. The SWNT is our example in the illustration of the idea because of the long-recognized outstanding potential of carbon nanotubes for applications in nanoscale sensor, devices, or machines [2]. We have observed that the

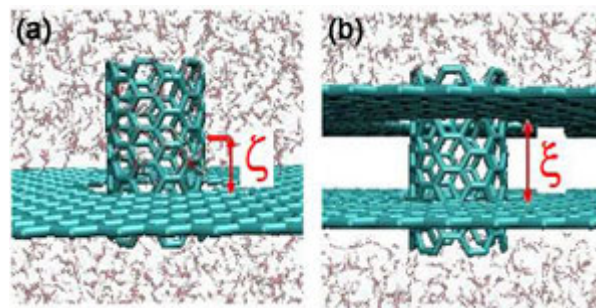


FIG. 1 (color online). Snapshots of the simulation systems. The dark green structures are the nanotube and the graphite sheet; the red and white pillars are representative of oxygen and hydrogen atoms in water molecules. (a) Side-view of the type 1 system. The red solid line denotes the position of the middle of the single-walled carbon nanotube. (b) Type 2 system. Two symmetrical sheets with a distance ξ ; there is a vacuum space between two sheets.

structure outside the nanochannel greatly affects water permeation across the nanochannel. The flux across the channel with an appropriate outside structure is approximately twice larger than the flux in the system with only a single carbon-sheet membrane.

Four types of systems were prepared. As shown in Fig. 1, an uncapped, armchair single-walled carbon nanotube [13] with 13.4 Å in length and 8.1 Å in diameter was embedded along the z direction in one or several graphite sheets. The system of the first type (type 1 system) had only one graphite sheet, as shown in Fig. 1(a). The distance between the graphite sheet and the middle of the SWNT is denoted as ζ . In the systems of the second type (type 2 systems) [see Fig. 1(b)], there were two carbon sheets with an equal distance from the nearest ends of the SWNT. The distance between those two sheets is denoted as ξ . There was no water molecule between the two sheets outside the SWNT. We also prepared the type 3 and 4 systems. In the type 3 system, three other graphite sheets fill the region between the two graphite sheets in the type 2 system with $\xi = 10.8$ Å. In the type 4 system, we used water molecules to fill the region. For the different systems, the pressures were initially set at the same value (for details, see supplementary material [14]).

Our simulations were performed with the GROMACS 3.3.2 molecular-dynamics program [15]. The solvent used was TIP3P water molecules [16]. The carbon-carbon interaction parameters were adopted from a previous work by Brenner [17] using the Tersoff formalism [18]. In the simulations, the carbon atoms were modeled as uncharged Lennard-Jones particles with a cross-section of $\sigma_{CC} = 0.34$ nm and $\sigma_{CO} = 0.3275$ nm and a depth of the potential well of $\epsilon_{CC} = 0.3612$ kJ mol⁻¹ and $\epsilon_{CO} = 0.4802$ kJ mol⁻¹ [5]. The cutoff for the van der Waals interaction was 1 nm. The carbon atoms at the inlet and outlet were fixed to prevent the SWNT from being swept away in the simulations and the other atoms of the SWNT is flexible. Periodic boundary conditions were applied in all directions. The electrostatic interactions (referring only to water-water electrostatic interactions) were handled by the PME summation method [19] with a cutoff for real space of 1 nm. All simulations were carried out at a constant volume with box size dimensions of $L_x = 5.0$ nm, $L_y = 5.0$ nm, $L_z = 5.0$ nm, and temperature = 300 K.

Following the method proposed by Zhu *et al.* [20], we applied an additional acceleration of 0.01 nm ps⁻² to each water molecule along $+z$ direction to obtain a pressure difference about 15 MPa between two ends of the SWNT.

For each system, we performed a 120-ns molecular-dynamics simulation and collected information from the last 110 ns of the simulation for analysis. For easy discussion, we define the flow as the total number of water molecules per nanosecond that leaves the SWNT from one end, having entered the opposite side. Similarly, the net flux is the difference between the number of water mole-

cules per nanosecond leaving from one end and the other (again having entered from the opposite end) [7,8]. To characterize the dipole orientation of the water chain, we computed the average angle $\bar{\phi}$, where ϕ is the angle between a water dipole at position Z inside the SWNT and the nanotube axis. The average covers all the water molecules inside the tube. As described in our previous papers [7], $\bar{\phi}$ falls into two ranges, $15^\circ < \bar{\phi} < 50^\circ$ and $130^\circ < \bar{\phi} < 165^\circ$. If we define a flip as $\bar{\phi}$ passing through 90° , we can compute the number of flips per nanosecond, denoted by the flipping frequency f_{flip} [7].

Figures 2(a) and 2(b) displays the water flow and flux, together with the flipping frequency for the type 1, type 2, type 3, and type 4 systems. In the type 1 system with $\zeta = 0$, the average flow and flux are 20.1/ns and 10.3/ns, respectively. The flow, flux and f_{flip} fluctuate only about 1% when ζ is changed; hereafter we use the type 1 system with $\zeta = 0$. For the type 2 systems, the larger distance between two sheets represents larger flux and flow. It is clear that the distance between the two sheets plays an important role in water flow and net flux across the

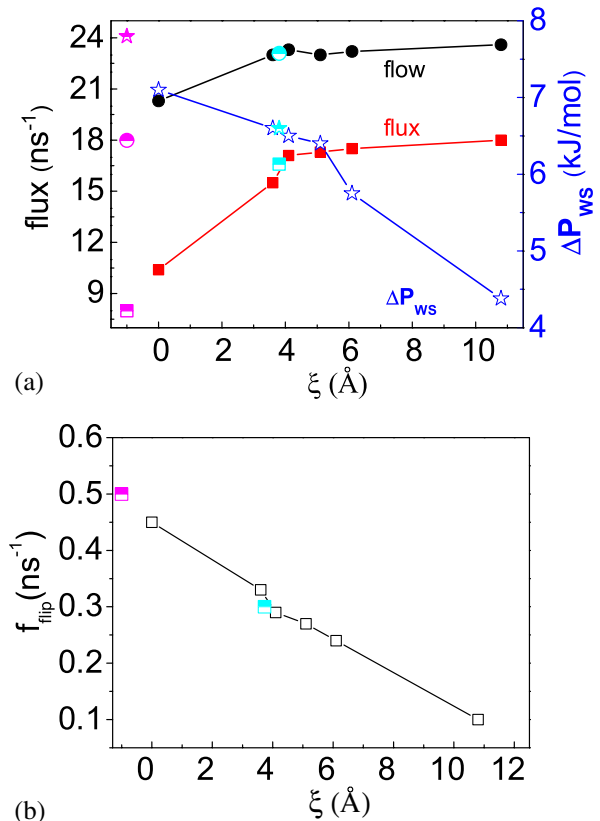


FIG. 2 (color online). Water flow, flux, and the depth of the potential barrier ΔP_{ws} (a) and Flip frequency f_{flip} (b) for the system of type 1 with $\zeta = 0$ and different systems of type 2, respectively. For simplicity, the points at $\xi = 0$ correspond to the type 1 system with $\zeta = 0$. In (a), the flow, flux and ΔP_{ws} of type 3 (in magenta) and type 4 (in cyan) are shown as half-filled circle, square, and star. In (b), the f_{flip} is in magenta and cyan, respectively.

channel, as well as the flipping frequency. As shown in Fig. 2(a), the flow and flux of the type 2 systems are larger than those observed in the type 1 system. As ξ decreases, the flow and flux decrease, while the change in f_{flip} exhibits the opposite behavior. The fluxes for the type 3 and 4 systems are 16.6/ns and 8.0/ns, respectively. The type 4 system has the most minimal flux among the simulated systems.

To understand the mechanism underlying the numerical observations, we have calculated the average interaction potentials, P_{WS} , of water molecules at position Z inside the SWNT with water molecules outside the channel in the membrane region, carbon nanotube, and carbon sheets. The membrane region is defined as the region with position $-6.7 \text{ \AA} < z < 6.7 \text{ \AA}$, i.e., the space between the two ends of the SWNT, as displayed in Fig. 1. Figure 3(a) shows that the potential profiles are symmetric with respect to the center of the carbon nanotube ($z = 0$) and the absolute value of P_{WS} increases when more water molecules surround the carbon nanotube except for the type 4 system. The type 4 system has the largest absolute value of P_{WS} , and for the type 2 system the smaller value of ξ corresponds to the larger absolute value of P_{WS} .

The depth of the potential barrier, denoted by ΔP_{WS} , which is the difference between the maximum and minimum of the interaction potential profile of P_{WS} , is calculated and usually used to characterize the potential profile. The potential barriers ΔP_{WS} for the type 1 system and as a function of ξ for the type 2 system are plotted as blue stars in Fig. 2(a). It is evident that with more water molecules which correspond to a deeper potential well, the resultant smaller flow and flux are induced. We further quantitatively study the relationship of the flow and net flux with respect to the depth of the barrier ΔP_{WS} for all the systems as shown in Fig. 3(b). It likewise demonstrates that a smaller potential barrier corresponds to a larger flux. However, the flux does not show an exponential decay, implying that the flux may not be solely governed by the potential barrier.

We have further computed the average velocities of the water molecules with a distance of less than 3 \AA from any atom of the SWNT in the membrane region outside the nanochannel for the type 1 and 2 systems. It was found that the average velocity is about 0.75 m/s for the type 1 system, and 0.43 m/s , 0.28 m/s and 0.22 m/s for the type 2 system with $\xi = 3.6, 4.1$, and 5.1 \AA , respectively, along the flux direction of water molecules inside the channel. It is clear that the smaller the value of flux inside the nanopore, the larger is the average velocity of the water molecules of the first layer outside the nanochannel. The water molecules in the membrane region outside the channel are driven along by the water flowing inside the tube, which affects the movement of the water inside.

In summary, unlike the macroscopic scenario, the structure outside a nanochannel has an important impact on water permeation across the nanochannel. The water net flux across the channel with an appropriate outside struc-

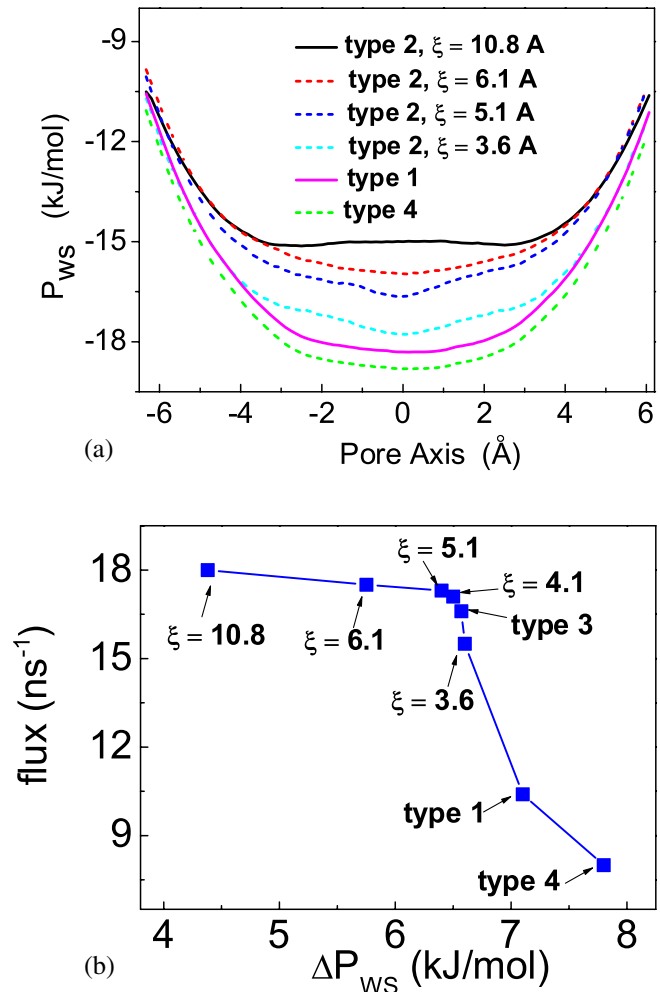


FIG. 3 (color online). Interactions P_{WS} between water inside the SWNT and water outside the channel in the membrane region, carbon nanotube, and carbon sheets in the membrane region, in a type 1 system with $\xi = 0 \text{ \AA}$ (magenta); type 2 systems with $\xi = 3.6 \text{ \AA}$ (cyan), 5.1 \AA (blue), 6.1 \AA (red) and 10.8 \AA (black); type 4 system (green), respectively, (A). Relationship of the net flux with the depth of the barrier ΔP_{WS} in the potential profiles (B).

ture is about twice larger than the flux in the system with only a single carbon-sheet membrane. This is due to the interactions between the water inside the single-walled channel and other molecules outside the nanochannel, which reduces the movement of the water molecules inside the nanotube. Thus, as more molecules surround the carbon nanotube, there is a lesser water flux across the nanotube. It is noteworthy that in practical nanochannel applications, if the nanochannels are semiconductors [21], the screen effect should be considered, and the electrostatic interactions of the water molecules inside and outside the nanochannel will decrease, thereby reducing the effect of the outside structure.

Our findings may be helpful in the design of high-flux nanochannels and for the provision of insights into the contribution of the lipid membrane to water permeation

across biological water channels. Moreover, the results indicate that the water permeation across a single-walled nanochannel may have significant differences from the water permeation across a multiwalled nanochannel.

We thank Dr. Zijian Xu and Houhui Yi for helpful discussions and comments. X.G. thanks Professors Ke Xu and Hui Yang for generous help. This work was supported by grants from NNSFC under No. 10674146 and No. 10825520, the National Basic Research Program under No. 2006CB936000 and Shanghai Supercomputer Center of China. H.P. acknowledges the partial support from the Institute for Mathematical Sciences, National University of Singapore.

*fanghaiping@sinap.ac.cn

- [1] K. Murata *et al.*, Nature (London) **407**, 599 (2000); B. L. de Groot and H. Grubmüller, Science **294**, 2353 (2001); E. Tajkhorshid *et al.*, Science **296**, 525 (2002).
- [2] G.M. Whitesides, Nature (London) **442**, 368 (2006); H. Craighead, Nature (London) **442**, 387 (2006); T.M. Squires and S.R. Quake, Rev. Mod. Phys. **77**, 977 (2005); B. Bourlon, J. Wong, C. Miko, L. Forro, and M. Bockrath, Nature Nanotech. **2**, 104 (2007); S. Ghosh, A.K. Sood, and N. Kumar, Science **299**, 1042 (2003); K. Besteman, J.O. Lee, F.G.M. Wiertz, H.A. Heering, and C. Dekker, Nano Lett. **3**, 727 (2003).
- [3] J.K. Holt *et al.*, Science **312**, 1034 (2006).
- [4] R.F. Service, Science **313**, 1088 (2006).
- [5] G. Hummer, J.C. Rasaiah, and J.P. Noworyta, Nature (London) **414**, 188 (2001).
- [6] O. Beckstein, P.C. Biggin, and M.S.P. Sansom, J. Phys. Chem. B **105**, 12902 (2001); F.Q. Zhu and K. Schulten, Biophys. J. **85**, 236 (2003).
- [7] R.Z. Wan, J.Y. Li, H.J. Lu, and H.P. Fang, J. Am. Chem. Soc. **127**, 7166 (2005).
- [8] J.Y. Li, X.J. Gong, H.J. Lu, D. Li, H.P. Fang, and R.H. Zhou, Proc. Natl. Acad. Sci. U.S.A. **104**, 3687 (2007); X.J. Gong, J.Y. Li, H.J. Lu, R.Z. Wan, J.C. Li, J. Hu, and H.P. Fang, Nature Nanotech. **2**, 709 (2007).
- [9] A.V. Raghunathan and N.R. Aluru, Phys. Rev. Lett. **97**, 024501 (2006); P. Gallo, M. Rovere, and E. Spohr, J. Chem. Phys. **113**, 11324 (2000); L. Kullman, M. Winterhalter, and S.M. Bezrukov, Biophys. J. **82**, 803 (2002).
- [10] M. Whitby and N. Quirk, Nature Nanotech. **2**, 87 (2007).
- [11] R.H. Zhou, X.H. Huang, C.J. Margulis, and B.J. Berne, Science **305**, 1605 (2004); K. Koga, G.T. Gao, H. Tanaka, and X.C. Zeng, Nature (London) **412**, 802 (2001); G. Reiter *et al.*, Phys. Rev. Lett. **97**, 247801 (2006); M. Majumder, N. Chopra, R. Andrews, and B.J. Hinds, Nature (London) **438**, 44 (2005); L. Sun and R. Crooks, J. Am. Chem. Soc. **122**, 12340 (2000); R. Allen, S. Melchionna, and J.P. Hansen, Phys. Rev. Lett. **89**, 175502 (2002); W.H. Noon, K.D. Ausman, R.E. Smalley, and J.P. Ma, Chem. Phys. Lett. **355**, 445 (2002).
- [12] B.Y. Wang and P. Kral, J. Am. Chem. Soc. **128**, 15984 (2006).
- [13] J. Liu *et al.*, Science **280**, 1253 (1998).
- [14] See EPAPS Document No. E-PRLTAO-101-079850 for supplementary material. For more information on EPAPS, see <http://www.aip.org/pubservs/epaps.html>.
- [15] B. Hess *et al.*, Gromacs-3.3 (Department of Biophysical Chemistry, University of Groningen, Groningen, 2005).
- [16] W.L. Jorgensen, J. Chandrasekhar, J.D. Madura, R.W. Impey, and M.L. Klein, J. Chem. Phys. **79**, 926 (1983).
- [17] D.W. Brenner, Phys. Rev. B **42**, 9458 (1990).
- [18] J. Tersoff, Phys. Rev. Lett. **61**, 2879 (1988).
- [19] T.A. Darden, D.M. York, and L.G. Pedersen, J. Chem. Phys. **98**, 10089 (1993).
- [20] F.Q. Zhu, E. Tajkhorshid, and K. Schulten, Biophys. J. **83**, 154 (2002).
- [21] D.Y. Lu, Y. Li, S.V. Rotkin, U. Ravaioli, and K. Schulten, Nano Lett. **4**, 2383 (2004); B. Kozinsky and N. Marzari, Phys. Rev. Lett. **96**, 166801 (2006); F. Leonard and J. Tersoff, Appl. Phys. Lett. **81**, 4835 (2002).